J. Radiat. Res., 49, 133–146 (2008)

Regular Paper

Quantitative Analysis of Isolated and Clustered DNA Damage Induced by Gamma-rays, Carbon Ion Beams, and Iron Ion Beams

Hiroaki TERATO[1]*, Ruri TANAKA[1], Yusuke NAKAARAI[1], Tomonori NOHARA[1], Yusuke DOI[2], Shigenori IWAI[2], Ryoichi HIRAYAMA[3], Yoshiya FURUSAWA[3] and Hiroshi IDE[1]

Clustered DNA damage/Double-strand breaks/Oxidized base lesions/High LET radiation/Relative biological effectiveness (RBE).

Ionizing radiation induces multiple damaged sites (clustered damage) together with isolated lesions in DNA. Clustered damage consists of closely spaced lesions within a few helical turns of DNA and is considered to be crucial for understanding the biological consequences of ionizing radiation. In the present study, two types of DNA, supercoiled plasmid DNA and linear lambda DNA, were irradiated with γ-rays, carbon ion beams, and iron ion beams, and the spectra and yield of isolated DNA damage and bistranded clustered DNA damage were fully analyzed. Despite using different methods for damage analysis, the experiments with plasmid and lambda DNA gave largely consistent results. The spectra of both isolated and clustered damage were essentially independent of the quality of the ionizing radiation used for irradiation. The yields of clustered damage as well as of isolated damage decreased with the different radiation beams in the order γ > C > Fe, thus exhibiting an inverse correlation with LET [γ (0.2 keV/μm) < C (13 keV/μm) < Fe (200 keV/μm)]. Consistent with *in vitro* data, the yield of chromosomal DNA DSBs decreased with increasing LET in Chinese hamster cells irradiated with carbon ion beams with different LETs, suggesting that the decrease in the yield of clustered damage with increasing LET is not peculiar to *in vitro* irradiation of DNA, but is common for both *in vitro* and *in vivo* irradiation. These results suggest that the adverse biological effect of the ionizing radiation is not simply accounted for by the yield of clustered DNA damage, and that the complexity of the clustered damage needs to be considered to understand the biological consequences of ionizing radiation.

INTRODUCTION

Ionizing radiation causes damage to DNA in cells, thereby inducing mutations, neoplastic transformation, and cell death. Radiation-induced DNA damage is comprised of oxidized pyrimidine and purine base lesions, abasic sites, and strand breaks.[1)] These lesions are generated either as isolated lesions in DNA or as multiply damaged sites (clustered damage) which consist of closely spaced lesions within a few helical turns of the DNA molecule.[2–4)] The former type of DNA lesions commonly result from ionizing radiation and chemical oxidizing agents such as hydrogen peroxide, but the latter is unique to ionizing radiation since such radiation can induce multiple localized ionization events in molecules along its track. It has been suggested that clustered DNA damage is involved in the adverse biological effects of ionizing radiation. For instance, a double-strand break (DSB) comprised of two closely opposed single-strand breaks (SSBs) is a typical clustered damage, and cells deficient in DSB repair are indeed hypersentive to ionizing radiation.[5)] Another class of clustered DNA damage consists of clustered base damage comprising closely spaced lesions of different types, such as oxidized base damage, abasic sites, and SSBs.[6,7)] Previous studies have shown that the abortive repair of clustered base lesions on opposing DNA strands results in DSBs and can lead to adverse biological consequences, indicating a crucial role for clustered base damage

*Corresponding author: Phone: +81-82-424-7329,
Fax: +81-82-424-7458,
E-mail: hterato@hiroshima-u.ac.jp
[1]Department of Mathematical and Life Sciences, Graduate School of Science, Hiroshima University, Higashi-Hiroshima 739-8526, Japan; [2]Division of Chemistry, Graduate School of Engineering Science, Osaka University, Toyonaka 560-8531, Japan; [3]Heavy-Ion Radiobiology Research Group, Research Center for Charged Particle Therapy, National Institute of Radiobiological Sciences, Chiba 263-8555, Japan.
doi:10.1269/jrr.07089

together with DSBs.[8–11)]

High linear energy transfer (LET) radiation produces more severe biological consequences than does low LET radiation. In mammalian cells, the relative biological effectiveness (RBE) as measured by cell killing rises with increasing LET values up to 100–200 keV/μm, and then decreases due to an overkill effect. Considering that high LET radiation generates a denser ionization track than low LET radiation, it is possible that high LET radiation directly or indirectly produces detrimental clustered DNA damage more efficiently than low LET radiation, thereby resulting in severe biological consequences. Furthermore, dense ionization events associated with high LET radiation can increase the frequency of DNA lesions within a damage cluster, and increase the structural complexity of clustered DNA damage. Thus, the quantity and complexity of clustered DNA damage are two important but relatively poorly understood parameters which determine the severity of the effects of ionizing radiation. Currently the assessment of the structural complexity of clustered DNA damage relies largely on computational simulations,[12)] whereas the quantity of clustered DNA damage has been experimentally measured using ionizing radiation with various LET values. According to *in vivo* data, the RBE for chromosomal DNA DSB formation varies between 0.5 and 1.6 for radiation with various LET values, and this contrasts with values measured using other biological endpoints such as cell killing (RBE = 3.5–4) and mutation induction (RBE = 6–12).[13)] Also, although not necessarily clustered damage, the yields of oxidized base lesions in irradiated cells tend to decrease with increasing LET values.[14)] LET-dependent formation of DNA damage was also assessed *in vitro* by irradiation of supercoiled plasmid[15,16)] and linear T7 DNA[6,17)] using different analytical approaches (*i.e.*, conformational changes for plasmids, and size dispersion for T7). Although these results unambiguously demonstrated the formation of oxidized base and abasic clusters together with DSBs in irradiated DNA, the spectra and yields of clustered damage together with those of isolated damage have not been compared by using complete measurements of the relevant lesions.

In the present study, two types of DNA, supercoiled plasmid DNA and linear lambda DNA, were irradiated with γ-rays, and accelerated carbon and iron ions, and the resulting yields of isolated DNA damage and bistranded clustered DNA damage were analyzed. Despite using distinct methodologies for damage analysis, the experiments with plasmid and lambda DNA gave essentially consistent results. First, the spectra of neither isolated nor clustered damage were essentially dependent on the quality of ionizing radiation used. Second, the yields of clustered damage as well as the yields of isolated damage decreased with the different radiation in the order of γ > C > Fe, and hence showed an inverse correlation with LET values [γ (0.2 keV/μm) < C (13 keV/μm) < Fe (200 keV/μm)]. Moreover, consistent with this observation, the yield of chromosomal DNA DSBs decreased with increasing LET values in Chinese hamster cells irradiated with carbon ion beams of different LET values, suggesting that the decrease in the yield of clustered damage with increasing LET is not peculiar to the *in vitro* irradiation of DNA. These results suggest that the yield of clustered DNA damage does not account for the detrimental biological consequences of the ionizing radiation, and that it is crucial to consider the structural complexity of clustered damage to understand the biological consequences of ionizing radiation.

MATERIALS AND METHODS

Materials

pDEL19 plasmid DNA (4,814 bp) (Wako Chemicals) was amplified in *Escherichia coli* HB101 and purified with a Qiagen plasmid extraction kit. The purified plasmid was primarily of (> 95%) Type I supercoiled form. Lambda DNA (48,502 bp) was purchased from Nippon Gene. *E. coli* endonuclease (Endo) III, formamidopyrmidine-DNA glycosylase (Fpg), and human 8-oxoguanine-DNA glycosylase (OGG1) were prepared as previously reported.[18,19)] Agarose S (Nippon Gene) was used for conventional gel electrophoresis of plasmid DNA. Pulse field gel certified agarose (Bio-Rad) was used for pulse field gel electrophoresis (PFGE) and static field gel electrophoresis (SFGE). Aldehyde reactive probe (ARP) was obtained from Dojin Chemicals. Oligonucleotides containing thymine glycol (Tg) and 7,8-dihydro-8-oxoguanine (8-oxoG) were synthesized and purified as previously reported.[18–20)]

Irradiation of DNA

pDEL19 DNA and lambda DNA (both at a concentration of 400 μg/ml) were dissolved in 10 mM Tris-HCl (pH 7.5) and irradiated in polypropylene microtubes with ^{60}Co γ-rays and accelerated carbon (290 MeV/amu) and iron (500 MeV/amu) ions at room temperature under aerobic conditions. The LET values were 0.2 (γ-rays), 13 (carbon), and 200 (iron) keV/μm. Carbon ion beams with other LET values (30 and 50 keV/μm) were generated using appropriate binary filters placed in the incident beam line and used for the irradiation of cells. γ-Irradiation was performed with a ^{60}Co γ-ray source in the Faculty of Engineering, Hiroshima University. The dose rate was calibrated with Fricke dosimetry. Irradiation with carbon and iron ion beams was done at the Heavy Ion Medical Accelerator in Chiba (HIMAC) at the National Institute of Radiobiological Sciences. Dose rates were 4 Gy/min for γ-rays and carbon ions, and 15 Gy/min for iron ions. Irradiated DNA was quickly frozen and stored at –80°C until analysis.

Damage analysis of plasmid DNA

DNA damage induced in pDEL19 plasmid DNA was ana-

lyzed by observing conformational changes to the DNA. Formations of a SSB and a DSB convert supercoiled DNA (Type I) to nicked circular (Type II) and linear (Type III) DNA, respectively. Oxidized base lesions were analyzed using Endo III and Fpg, which remove primarily oxidized pyrimidine and purine lesions, respectively, from DNA, and concomitantly incise resulting abasic sites. Although these glycosylases are not completely specific for purine- or pyrimidine-derived lesions, particularly when used in huge excess, the formation of Type II and Type III DNA after treatment with Endo III reveals the approximate yields of isolated and clustered oxidized pyrimidine lesions, respectively. Similarly treatment with Fpg reveals those of isolated and clustered oxidized purine lesions. Irradiated pDEL19 DNA (100 ng) was incubated with 40 ng of Endo III or Fpg in 10 mM Tris-HCl (pH 7.5), 1mM EDTA, and 100 mM NaCl at 37°C for 1 h. The ratio of plasmid DNA and glycosylases (Endo III and Fpg) was determined in preliminary titration experiments to ensure exhaustive digestion of irradiated DNA (data not shown). Irradiated DNA (50 ng) with or without enzyme treatments were added to a gel loading solution (0.25% bromophenol blue, 30% glycerol, and 1 mM EDTA) and DNA was separated on a standard 0.8% agarose gel prestained with ethidium bromide (EtBr) in TAE buffer (40 mM Tris, 40 mM acetic acid, and 1 mM EDTA) at 50 V for 105 min. The gel was then imaged on a FAS II system (Toyobo), and Type I–III bands were quantified with NIH Image gel plotting macro software.

The yields, SSB_i (sites/Gy/10^6 bp), of isolated damage including prompt SSBs (SSB_P) and SSBs induced by Endo III (SSB_E) and Fpg (SSB_F) were determined with equation 1, assuming a single hit model and a Poisson distribution of lesions, where D_{37} is the dose (Gy) required to give an average of 1 SSB per pDEL19 molecule (4814 bp).

$$SSB_i = 10^6 / (D_{37} \times 4814) \quad \text{(where i = P, E, or F is defined above)} \qquad \text{eq. 1}$$

The yields of oxidized pyrimidine and purine lesions were calculated with equations 2 and 3, respectively.

$$\text{oxidized pyrimidines} = SSB_E - SSB_P \qquad \text{eq. 2}$$
$$\text{oxidized purines} = SSB_F - SSB_P \qquad \text{eq. 3}$$

The yields (sites/Gy/10^6 bp) of clustered damage including prompt DSBs (DSB_P) and DSBs induced by Endo III (DSB_E) and Fpg (DSB_F) were determined from linear regression analysis of the slopes of dose response plots for the formation of Type III DNA. The yields of oxidized pyrimidine and purine clusters were calculated by equations 4 and 5, respectively.

$$\text{oxidized pyrimidne clusters} = DSB_E - DSB_P \qquad \text{eq. 4}$$
$$\text{oxidized purine clusters} = DSB_F - DSB_P \qquad \text{eq. 5}$$

Damage analysis of lambda DNA

Clustered DNA damage in lambda DNA was analyzed from the size changes of irradiated DNA (DSBs) and size changes resulting from subsequent glycosylase treatments (oxidized base clusters). The numbers of DSBs and oxidized base clusters were calculated from the number average length of the DNA fragments.[21] For analysis of oxidized pyrimidine and purine clusters, irradiated DNA (2 μg) was treated with 0.2 μg of Endo III and Fpg, respectively, at 37°C for 1 h before electrophoresis. This converted oxidized pyrimidine and purine clusters to DSBs. The ratio of lambda DNA to glycosylases (Endo III and Fpg) was determined in preliminary titration experiments to ensure exhaustive digestion of irradiated DNA (data not shown). Irradiated DNA (20 ng), with or without enzyme treatment, was added to a gel loading solution (0.05% bromophenol blue, 0.05% xylene cyanol, 6% glycerol, and 2 mM EDTA) and separated with PFGE. Electrophoresis was performed using a 1% agarose gel in 0.5 × TBE (44.5 mM Tris, 44.5 mM boric acid, and 1 mM EDTA) at 14°C on a CHEF-DRII apparatus (BioRad) equipped with a buffer cooling system. The initial voltage was 6 V (current ~115 mA) and the pulse time was increased linearly from 0.1 to 2.5 s for a period of 8 h. DNA size markers (8.3–48.5 kbp, BioRad) were also run side by side to calibrate fragment sizes. After electrophoresis, the gel was stained in 0.5 × TBE containing 0.3 μg/ml EtBr for 20 min and washed twice with 0.5 × TBE. The gel was imaged on a FAS II system, and the dispersion of DNA fragments was analyzed with NIH Image gel plotting macro software. The number average length of DNA fragments associated with prompt DSBs (L_P), Endo III treatment (L_E), and Fpg treatment (L_F) at a given dose was calculated using Deltagraph Ver. 5. The yields (sites/Gy/10^6 bp) of clustered damage including prompt DSBs and oxidized pyrmidine and purine clusters were calculated with equations 6–8, respectively, where L_0 is the number average length of unirradiated DNA:

$$DSB = (1/L_P - 1/L_0) \times 10^6 \qquad \text{eq. 6}$$
$$\text{oxidized pyrimdine clusters} = (1/L_E - 1/L_P) \times 10^6 \qquad \text{eq. 7}$$
$$\text{oxidized purine clusters} = (1/L_F - 1/L_P) \times 10^6 \qquad \text{eq. 8}$$

Isolated DNA damage in lambda DNA was analyzed with the aldehyde reactive probe (ARP) assay in combination with Endo III and OGG1 (not Fpg) treatment as reported previously.[22,23] Although both Fpg and OGG1 remove oxidized purine bases and incise DNA, OGG1 (but not Fpg) leaves abasic sugar residues which are essential for the ARP assay. In the ARP assay, prompt abasic sites and those resulting from oxidized pyrimidines and purines by Endo III and OGG1 treatments, respectively, were specifically tagged with biotin-conjugated ARP and quantified with chemiluminescence using an avidin-biotin-horseradish peroxidase system. Thus, the assay without enzyme treatment reveals abasic sites, whereas those with Endo III and OGG1 reveal oxidized pyrimidine and purine lesions, respectively. It is

noted that in view of the reactivity of ARP, sites detected as prompt abasic sites by ARP would include, together with pure abasic sites, 3'-glycolaldehyde (fragmented sugar) and 2'-deoxyribonolactone (oxidized abasic site) but not 3'-glycolate (fragmented sugar). However, currently no comparative data are available as to how much pure abasic sites, 3'-glycolaldehyde, and 2'-deoxyribonolactone are produced by ionizing radiation. None the less, these lesions are sites where bases are missing (*i.e.*, abasic sites in a broad sense). For this reason and convenience, we tentatively bracketed them as abasic sites in this work.

Activity assays with Endo III and Fpg for oligonucleotide substrates containing clustered base damage

DNA substrates containing defined clustered base damage were constructed as follows. Top and bottom strands (both 31-mer) were 5'-end labeled using T4 polynucleotide kinase (Toyobo) and [γ-^{32}P]ATP (166.5 TBq/mmol, MP Biomedicals) and purified by spin columns. The specific radioactivities of top and bottom strands were adjusted to be equal by adding the corresponding unlabeled strands, and final the two strands were annealed at an equimolar ratio. The substrates contained two residues of Tg for Tg/Tg clusters or two residues of 8-oxoG for 8-oxoG/8-oxoG clusters. One lesion was placed between the –5 and +5 positions in the top strand, and the other was at position B in the bottom strand (see Fig. 4A). Ten nM of substrates containing clustered damage were incubated with 10–1000 nM Endo III or Fpg in 10 mM Tris-HCl (pH 7.5), 1 mM EDTA, 100 mM NaCl, 0.1 mg/ml BSA, and 0.005% Tween 20 (total volume 10 µl) at 37°C for 1 h. After digestion, the sample was mixed with an equal volume of gel loading solution (0.05% xylene cyanol, 0.05% bromophenol blue, 20 mM EDTA, and 98% formamide), heat denatured, and separated with 16% denaturing polyacrylamide gel electrophoresis (PAGE). The radioactivity of the gel was quantified with a Fuji BAS2000 phosphorimaging analyzer.

Analysis of chromosomal DNA DSBs in irradiated cells

Chinese hamster ovary AA8 cells were seeded at a concentration of 1×10^4 cells per flask and cultured in minimum essential alpha medium (Gibco) supplemented with 10% fetal bovine serum in a 5% CO_2 atmosphere at 37°C for 24 h prior to irradiation. The cells were irradiated with γ-rays and carbon or iron ion beams at 4°C using a temperature controlled apparatus. After irradiation, cells were washed twice with ice-cold phosphate buffered saline (PBS), suspended in cold PBS containing 0.2% trypsin, and kept on ice for 20 min. Chromosomal DNA DSBs were analyzed with SFGE.[24,25] The harvested cells were embedded in 1% agarose gel plugs (Cambrex, SeaPlaque GTG agarose). The plugs were incubated in lysis buffer (Trevigen, #4250-050-01) containing 0.5 mg/ml proteinase K (Sigma) at 50°C for 24 h, and then rinsed in TE buffer [10 mM Tris-HCl (pH 8.0) and 1 mM EDTA] at room temperature for 1 h. The plugs were then inserted into slot well in the 0.6% agarose gel, and electrophoresis was performed at 0.6 V/cm in TBE for 27 h. The gel was stained with EtBr and the image was analyzed as described for plasmid DNA. The formation of chromosomal DNA DSBs was analyzed using the fraction of activity released (FAR) assay with equation 9, where DNA_1 and DNA_2 denote the amounts of DNA retained in and eluted from the well, respectively.

$$\text{FAR } (\%) = DNA_2/(DNA_1 + DNA_2) \times 100 \qquad \text{eq. 9}$$

To measure cell survival, cells were irradiated at room temperature, recovered with trypsinization, and seeded in fresh media at appropriate dilutions. After incubation for 9–10 days, cells were fixed with 10% formalin and stained with 1% methylene blue. The number of colonies appearing was counted.

RESULTS

Formation of isolated and clustered damage in supercoiled plasmid DNA

pDEL19 plasmid DNA was irradiated with γ-rays and carbon and iron ion beams in 10 mM Tris-HCl, and conformational changes from Type I (supercoil) to Type II (nicked circular) and Type III (linear) were analyzed with agarose gel electrophoresis (data not shown). With the three types of radiation used, the fraction of Type I DNA was seen to decrease exponentially with increasing dose, showing single hit kinetics (Figs. 1A–1C). The post-treatment of irradiated DNA with Endo III or Fpg lead to a further decrease of Type I DNA, indicating the presence of oxidized base lesions in the irradiated DNA. The yields (sites/Gy/10^6 bp) of isolated damage including prompt SSBs and oxidized pyrimidine and purine lesions were determined from the D_{37} dose (see Materials and Methods) and are summarized in Table 1. The yields of the individual components comprising the isolated damage (SSBs, oxidized pyrimidines, and oxidized purines) were present in quantities of 1.40–4.35 per Gy per 10^6 bp and decreased with the different radiation beams in the order $\gamma > C > Fe$. The total yields of isolated damage decreased in the same order (Fig. 2A). The yields of clustered damage were analyzed from the formation of Type III DNA. With all types of radiation used, the Type III fraction increased almost linearly with dose, and post-treatment of irradiated DNA with Endo III or Fpg resulted in further increases in the Type III fraction (Figs. 1D–1F), indicating the formation of oxidized base clusters in irradiated DNA. The yields of clustered damage, including prompt DSBs and oxidized pyrimidine and purine clusters, were determined from the slopes of the dose response plots (see Materials and Methods) and are summarized in Table 1. The yields of individual components of clustered damage (DSBs, oxidized pyrimidine clusters, and oxidized purine clusters) were in

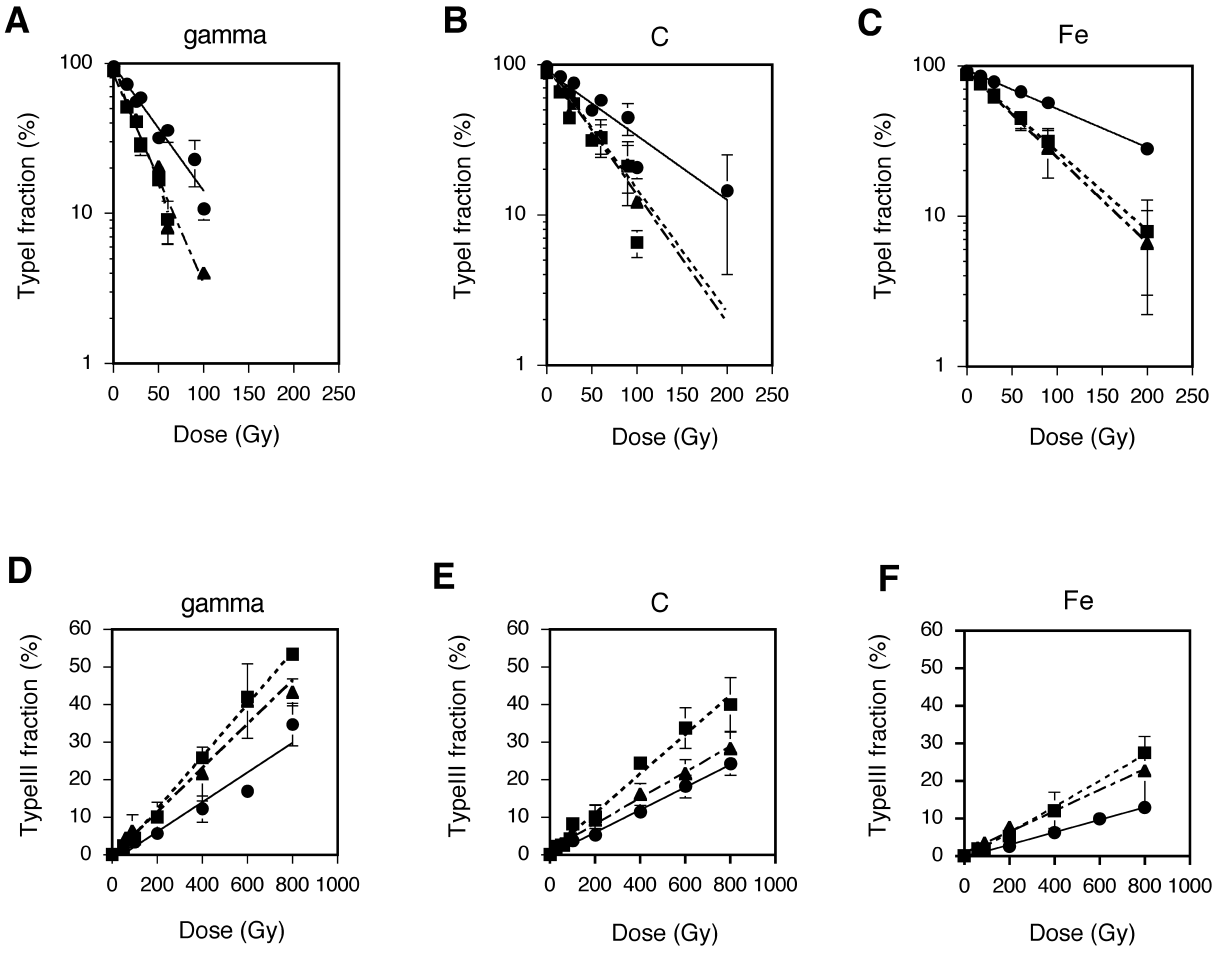

Fig. 1. Dose response plots showing the fractions of supercoiled (Type I) and linear DNA (Type III). Supercoiled pDEL19 DNA (400 μg/ml) was irradiated in 10 mM Tris-HCl (pH 7.5) with γ-rays (A and D), carbon ion (B and E), and iron ion (C and F) beams. After irradiation, DNA was untreated (circles with solid lines) or incubated with Endo III (squares with broken lines) or Fpg (triangles with chain lines). Type I and Type III fractions were analyzed with agarose gel electrophoresis as described in Materials and Methods. Data are means ± standard deviations from 5 independent experiments.

the range of 2.0–8.3 per Gy per 10^8 bp and approximately two orders of magnitude lower than that seen for isolated damage. The yields of the individual components of clustered damage tended to decrease with the different radiations in the order γ > C > Fe. A similar tendency was observed for total yields of clustered damage (Fig. 2B). Although the statistical significance was moderate ($p < 0.1$), the difference in the yields of total clustered damage was reproducibly observed for γ-rays, carbon ion, and iron ion beams in repeated experiments. The ratio of the yields of total clustered *versus* isolated damage was 1.5–1.9% and independent of the type of radiation used (Fig. 2C). Similarly, the spectra of clustered damage were essentially independent of the type of radiation, so that there were no significant differences in these spectra for γ-rays, carbon ions, and iron ions (Fig. 2E). The same was true for isolated damage (Fig. 2D). Oxidized base lesions were the dominating species of lesion, and accounted for 64–70% of isolated damage and for 54–62% of clustered damage.

Formation of isolated and clustered damage in linear lambda DNA

Lambda DNA was irradiated with γ-rays, carbon ion, and iron ion beams in 10 mM Tris-HCl and analyzed for isolated and clustered damage. The dose ranges used were similar to those used for plasmid DNA. For the analysis of isolated damage, a different approach from that used for plasmid DNA was utilized since break-associated conformational changes do not occur in linear DNA. Instead, prompt abasic sites (possibly including certain fragmented and oxidized sugars) and those derived from oxidized pyrimidines and purines after Endo III and OGG1 treatments, respectively, were analyzed with the ARP assay (see Materials and Methods). Accordingly, the spectra of isolated damage determined for lambda and plasmid DNA partially overlap (oxidized pyrimidines and purines) but not completely

Table 1. Yields of isolated and clustered damage in pDEL19 plasmid DNA irradiated with various types of radiation

Damage	Yields (sites/10^6 bp/Gy)*		
	gamma	carbon	iron
Isolated damage			
SSBs	4.35 ± 0.79	2.68 ± 0.49	1.40 ± 0.14
oxidized pyrimidines	3.82 ± 0.38	2.50 ± 0.28	1.54 ± 0.31
oxidized purines	3.80 ± 0.63	2.13 ± 0.17	1.76 ± 0.43
total	11.97 ± 2.75	7.31 ± 0.89	4.70 ± 1.27
Clustered damage			
DSBs	0.083 ± 0.014	0.060 ± 0.005	0.034 ± 0.004
oxidized pyrimidine clusters	0.058 ± 0.003	0.050 ± 0.008	0.035 ± 0.004
oxidized purine clusters	0.038 ± 0.008	0.027 ± 0.007	0.020 ± 0.007
total	0.179 ± 0.044	0.137 ± 0.046	0.089 ± 0.022

*Data are means ± standard deviations from 5 independent experiments.

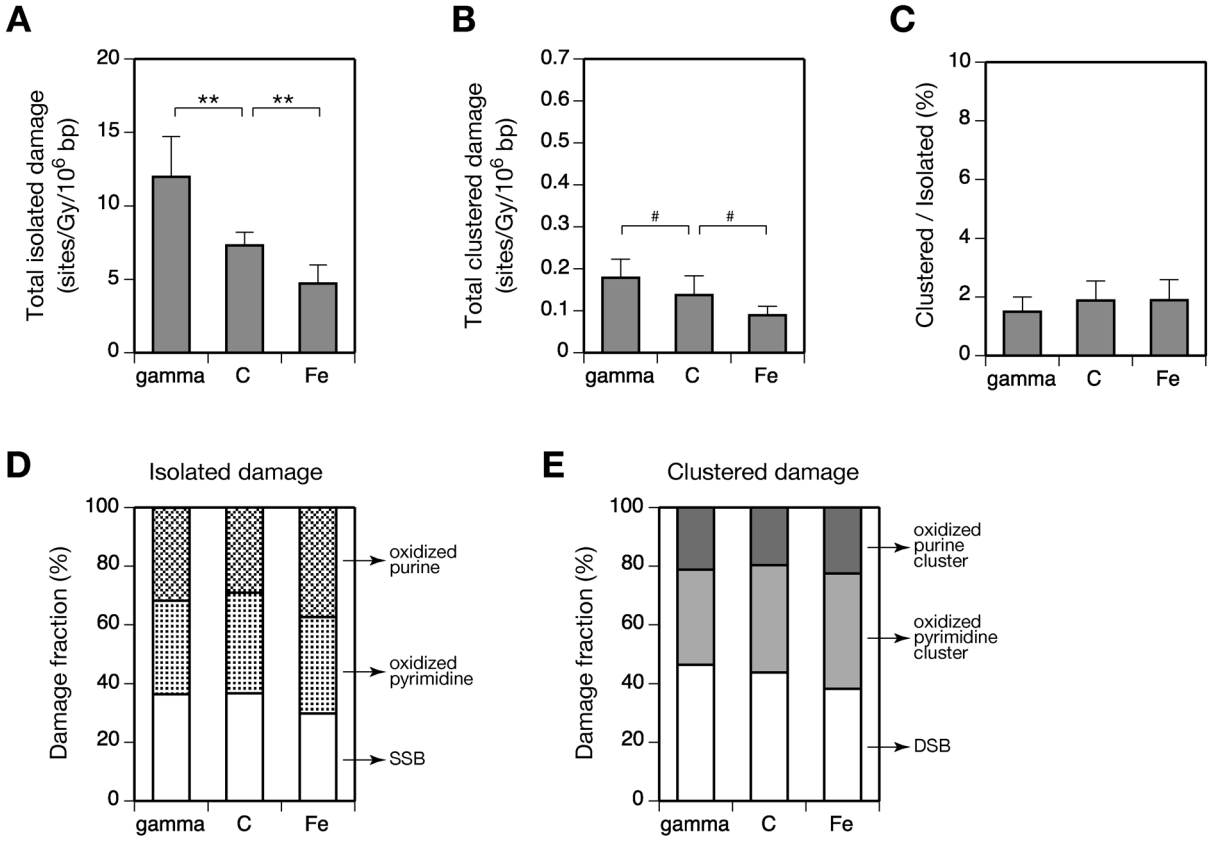

Fig. 2. Yields and spectra of isolated and clustered damage in pDEL19 plasmid DNA irradiated with γ-rays, carbon ion, and iron ion beams. Irradiation and analysis were performed as described in Fig. 1. A) Yields of total isolated damage (SSBs + oxidized pyrimidine and purine lesions). B) Yields of total clustered damage (DSBs + oxidized pyrimidine and purine clusters). C) Ratio of total clustered *versus* isolated damage. D) Spectra of isolated damage. E) Spectra of clustered damage. In panels A and B, statistical significance for the difference between adjacent bars is indicated by ** for $p < 0.01$ and # for $p < 0.1$ ($n = 5$).

Table 2. Yields of isolated and clustered damage in lambda DNA irradiated with various types of radiation

Damage	Yields (sites/10^6 bp/Gy)*		
	gamma	carbon	iron
Isolated damage			
abasic sites	6.04 ± 1.15	2.49 ± 0.71	1.24 ± 0.40
oxidized pyrimidines	3.09 ± 0.48	1.15 ± 0.31	0.82 ± 0.12
oxidized purines	5.41 ± 0.99	1.43 ± 0.28	1.13 ± 0.19
total	14.54 ± 3.14	5.07 ± 1.37	3.19 ± 0.30
Clustered damage			
DSBs	0.18 ± 0.03	0.11 ± 0.02	0.08 ± 0.02
oxidized pyrimidine clusters	0.24 ± 0.06	0.12 ± 0.03	0.09 ± 0.02
oxidized purine clusters	0.13 ± 0.04	0.09 ± 0.03	0.08 ± 0.01
total	0.55 ± 0.07	0.32 ± 0.03	0.25 ± 0.04

* Data are means ± standard deviations from 4 independent experiments.

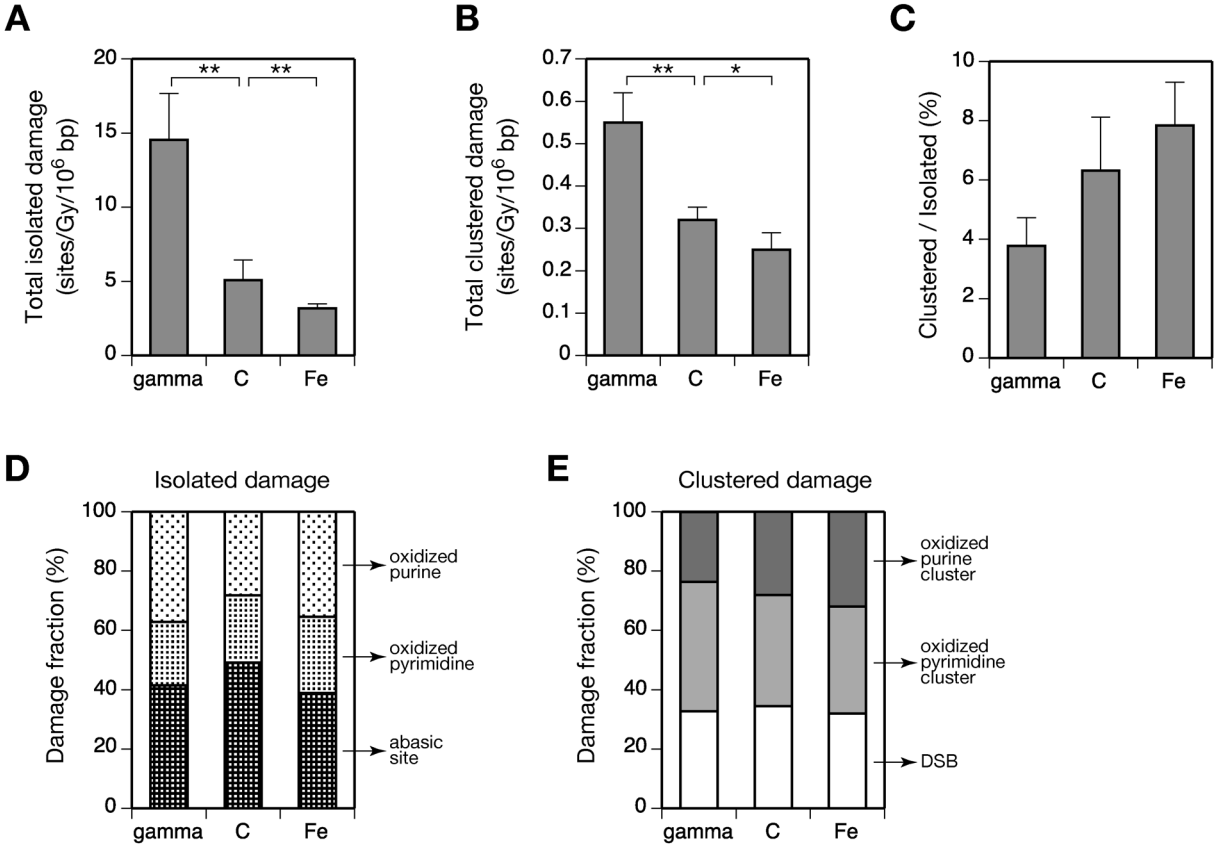

Fig. 3. Yields and spectra of isolated and clustered damage in lambda DNA irradiated with γ-rays, carbon ion, and iron ion beams. Irradiation, ARP assays for the quantitation of isolated damage, and analysis of the dispersion of DNA fragments for the quantitation of clustered damage were performed as described in Materials and Methods. A) Yields of total isolated damage (abasic sites + oxidized pyrimidine and purine lesions). B) Yields of total clustered damage (DSBs + oxidized pyrimidine and purine clusters). C) Ratio of total clustered *versus* isolated damage. D) Spectra of isolated damage. E) Spectra of clustered damage. In panels A and B, statistical significance for the difference between adjacent bars is indicated by ** for $p < 0.01$ and * for $p < 0.02$ ($n = 4$).

(abasic sites for lambda DNA *versus* SSBs for plasmid DNA). However, the sites measured as abasic sites by the ARP assay contain two types of damage including authentic baseless sites in undisrupted strands and dangling fragmented or oxidized sugar moieties at SSB ends.[23] Thus, the sites measured as abasic sites here contain SSBs, at least in part, although it is not clear to what extent these SSB-associated abasic sites comprise of the total number of abasic sites. Table 2 shows the yields of isolated damage for lambda DNA determined from dose response plots (not shown). The yields of individual isolated damage were in the range of 0.82–6.04 per Gy per 10^6 bp and are comparable to those in plasmid DNA. The variations of the yields of oxidized pyrimidines and purines for plasmid and lambda DNA were mostly less than two-fold. Furthermore, as seen in plasmid DNA, the yields of individual and total isolated damage decreased with the different radiations used in the order γ > C > Fe (Table 2 and Fig. 3A). Clustered damage was quantified by analysis of the number average length of DNA fragments resulting from prompt and glycosylase-induced DSBs (see Materials and Methods). The yield of clustered damage sites was in the range of 8–24 per Gy per 10^8 bp. As seen for isolated damage, the formation of individual and total clustered damage was radiation type-dependent and the yields decreased with the type of radiation in the order γ > C > Fe (Table 2 and Fig. 3B). Interestingly, despite measuring the same spectra of clustered damage (DSBs and oxidized pyrimidine and purine clusters), the total yield for lambda DNA was greater than that for plasmid DNA by 2–3-fold (Figs. 2B and 3B). Consequently, the ratio of total

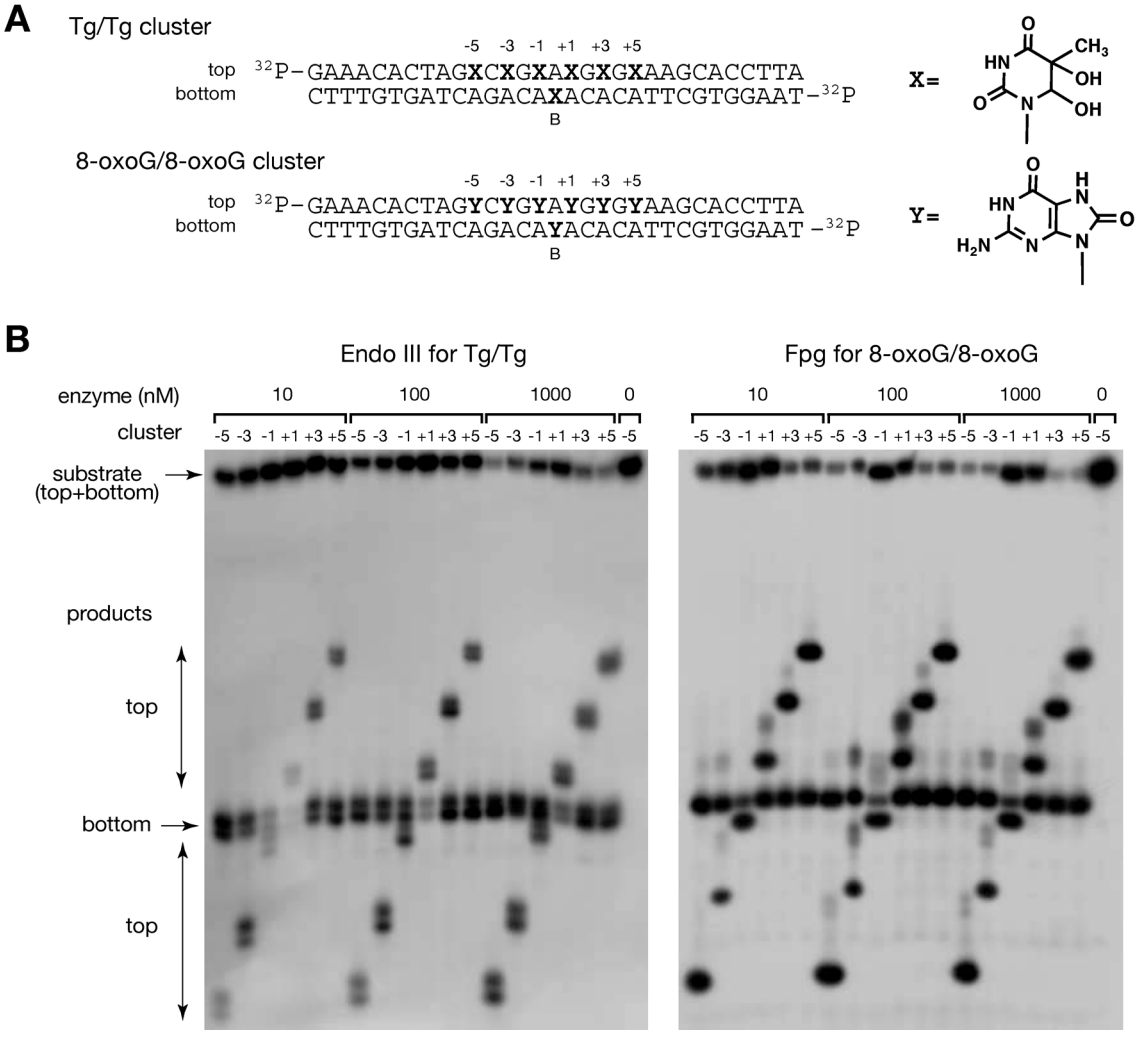

Fig. 4. PAGE analysis of the products resulting from the treatment of oligonucleotide substrates containing model clustered base damage with Endo III and Fpg. A) Sequence of substrates containing Tg/Tg or 8-oxoG/8-oxoG clusters. One lesion was placed between –5 and +5 in the top strand, and the other was at position B in the bottom strand. B) PAGE data for the substrates with different configurations of Tg/Tg and 8-oxoG/8-oxoG. The substrates (10 nM) were treated with the indicated concentrations of Endo III or Fpg at 37°C for 1h. The product bands resulting from the incision of the top and bottom strands are indicated by arrows.

clustered *versus* isolated damage was higher than that for plasmid DNA (Figs. 2C and 3C). Considering the damage spectra for isolated and clustered damage, there were no significant differences seen in those for γ-rays, carbon ions, and iron ions (Figs. 3D and 3E). With clustered damage, oxidized base clusters were dominant and constituted about 67% of the total clustered damage.

Activity of Endo III and Fpg on clustered base damage

To determine whether Endo III and Fpg can efficiently convert oxidized base clusters into DSBs in the present study, oligonucleotide substrates containing model Tg/Tg and 8-oxoG/8-oxoG clusters (Fig. 4A) were tested with the enzymes. Tg and 8-oxoG are ubiquitously formed in irradiated DNA. Figure 4B shows the results of product analysis with denaturing PAGE when substrates (10 nM) were treated with various concentrations of Endo III or Fpg (10, 100, and 1000 nM). The amount of incision products, from both the top and bottom strands, increased with increasing amounts of Endo III and Fpg. Figures 5A and 5B show the relationship between the yield of cleaved strands and the type of cluster when substrates were treated with a limited amount of enzyme (10 nM). With Tg/Tg clusters (Fig. 5A), the incision efficiency of the bottom strand decreased systematically with decreasing inter-lesion distance. The –1 cluster (two Tg residues at –1 and B), and the +1 cluster (two Tg residues at +1 and B) remained mostly intact under these conditions. The low activity of Endo III for these clusters indicates that the excision of the first Tg was impaired by a very close neighboring Tg. Unlike the bottom strand, the top strand was cleaved by Endo III inefficiently, implying a strand bias. Such an apparent strand bias was not observed when similar substrates containing a single Tg lesion in a top or bottom strand were treated with Endo III (Fig. S1 in supplementary material). Thus, the strand bias is characteristic to the substrates containing two Tg lesions (*i.e.*, clustered damages) that compete for Endo III. We have previously shown that Endo III exhibits a moderate sequence context preference upon excision of Tg and that the Tg flanked by two adenines (*i.e.*, A-Tg-A) is a preferred substrate for Endo III among those examined.[26] Since Tg in the bottom strand is embedded in this sequence context, it is inferred that the bottom

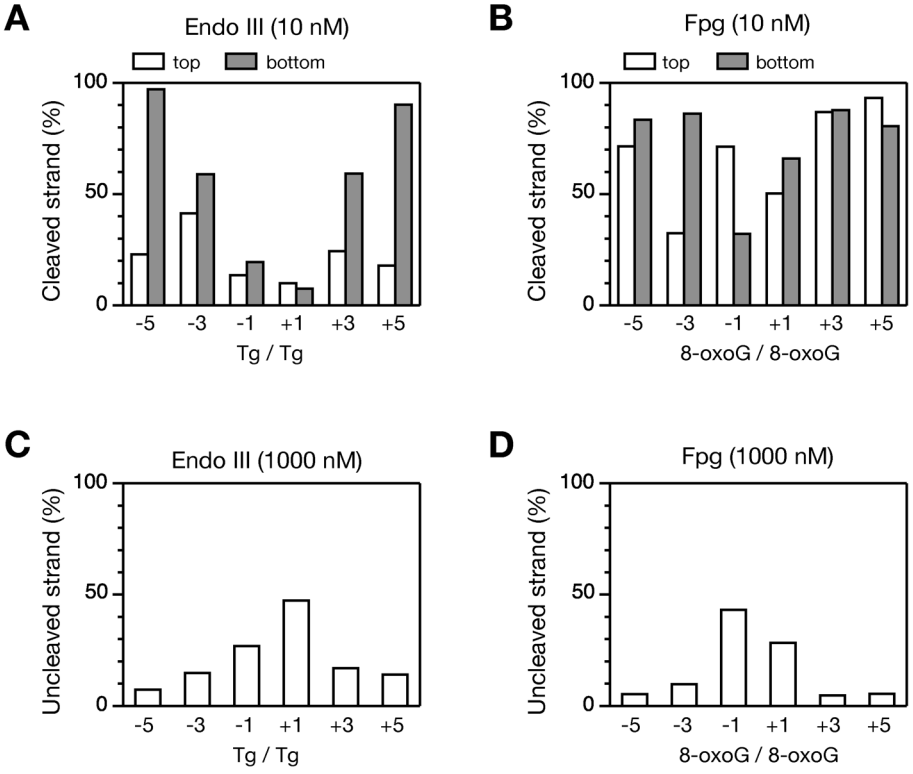

Fig. 5. Variations of the incision efficiencies of Endo III and Fpg for different types of Tg/Tg and 8-oxoG/8-oxoG clusters. Data are based on the quantitation of product bands in Fig. 4B. In the quantitation of cleaved strands, half the sum of all radioactivity in each lane was used as the total amount for each DNA strand since the top and bottom strands had the same specific radioactivities (see also Materials and Methods). A) Incision efficiency for the top and bottom strands containing Tg under limiting digestion conditions (Endo III = 10 nM). B) Incision efficiency for top and bottom strands containing 8-oxoG under limiting digestion conditions (Fpg = 10 nM). C) Fraction of uncleaved Tg strands (top + bottom) under exhaustive digestion conditions (Endo III = 1000 nM). D) Fraction of uncleaved 8-oxoG strands (top + bottom) under exhaustive digestion conditions (Fpg = 1000 nM).

strand was preferentially incised by Endo III compared to the top strand. The strand bias became increasingly apparent with increasing inter-lesion distance (±5 > ±3 > ±1) (Fig. 5A). In the case of the ±5 clusters that exhibited the strongest strand bias, it is possible that preferential cleavage of the bottom strand producing a SSB disrupted the way in which Endo III bound the DNA, though the exact reason remains elusive. Fpg cleaved 8-oxoG/8-oxoG clusters more efficiently than Endo III cleaved Tg/Tg clusters (Fig. 5B), but the inter-lesion distance-dependent variation as well as the strand bias of the cleavage efficiency were qualitatively similar to those for Endo III (Fig. 5A). Figures 5C and 5D show the percentage of uncleaved substrates (sum of top and bottom strands) after incubation with 1000 nM Endo III or Fpg, when the substrates were exhaustively digested. The molar ratio of the substrate and enzyme used here (substrate:enzyme = 1:100) is close to that used for the digestion of irradiated pDEL19 DNA, where the concentration of total clustered pymidine and purine damage was roughly 1 nM (calculated for γ-rays at 500 Gy from Table 1) and that for the enzyme was 165 nM (Endo III) and 130 nM (Fpg). Under these conditions, the top and bottom strands of –5, –3, +3, and +5 clusters were mostly (> 80%) incised by Endo III or Fpg, whereas those of the –1 and +1 clusters were more resistant to incision than other clusters. This result suggests that closely opposed base lesions except for –1 and +1 clusters can be effectively converted to DSBs by exhaustive digestion with Endo III or Fpg. The resistance of –1 and +1 clusters is likely due to the retardation of the activities of Endo III and Fpg, not for Tg/Tg or 8-oxoG/8-oxoG clusters, but instead for the reaction intermediates, which contain a base lesion (Tg or 8-oxoG) and a SSB, since either the top or bottom was mostly cleaved under these conditions. It has been shown that the excision of a base lesion by Endo III and Fpg is moderately retarded by a closely opposed base lesion, but more extensively retarded by a closely opposed SSB lesion.[27] Thus, radiation-induced clusters comprising two base lesions or a base lesion and a SSB with –1 and +1 configurations may not be converted efficiently into DSBs in the present analysis of irradiated DNA.

Formation of chromosomal DNA DSBs in irradiated cells

To elucidate the *in vivo* formation of clustered DNA damage, AA8 cells were irradiated with γ-rays, carbon ion, and iron ion beams (up to 20 Gy), and the formation of chromosomal DNA DSBs was analyzed with the FAR assay using SFGE. The irradiation and treatment of the cells before lysis was performed at 4°C to minimize DNA repair. With the three types of radiation used, chromosomal DNA from unirradiated cells was retained in the plug, but that from irradiated cells partially eluted into the gel, indicating the presence of chromosome fragmentation due to DSB formation (data not shown). The DNA fraction released into the gel increased almost linearly with increasing doses and the yield of the released DNA fraction (percent per Gy) was determined from the slope of the dose response plots. The yield of the released DNA fraction decreased with the different radiations used in the order γ > C > Fe (Fig. 6A). Conversely, consistent with known data, the cell killing efficiency of these radiations decreased in the order Fe > C > γ (Fig. 6B), showing a trend opposite to that for DSB formation. To clarify whether radiation quality has any influence on the yield of the released DNA fraction, similar experiments were performed using carbon ion beams with different LETs (13, 30, and 50 keV/μm). The yield of the released DNA fraction

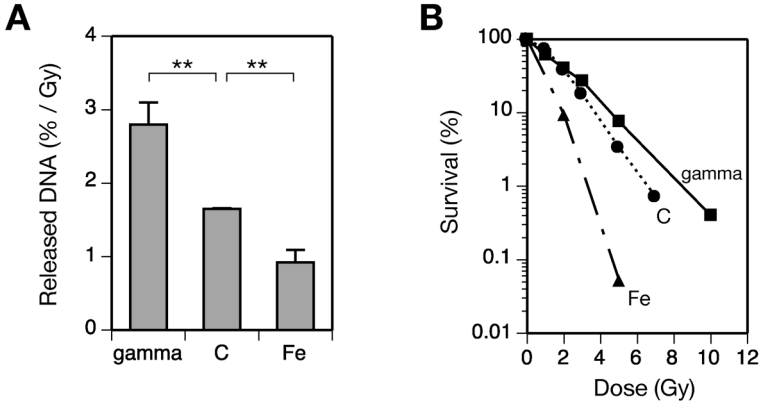

Fig. 6. Analysis of chromosomal DNA DSBs with FAR assays. Chinese hamster AA8 cells were irradiated at 4°C with γ-rays, carbon ion, and iron ion beams, and chromosomal DNA DSBs were analyzed with the FAR assays using SFGE as described in Materials and Methods. AA8 cells were also irradiated at room temperature and survival was measured with colony formation. A) Variation of the yield of released DNA with the different types of radiation. Statistical significance for the difference between adjacent bars were $p < 0.01$ ($n = 3$) and indicated by **. B) Cell survival after irradiation with γ-rays, carbon ion, and iron ion beams.

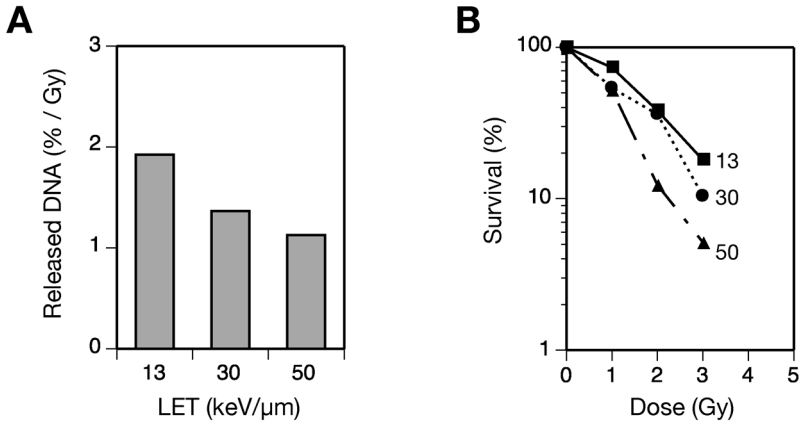

Fig. 7. Analysis of chromosomal DNA DSBs with the FAR assay. Chinese hamster AA8 cells were irradiated at 4°C with carbon ion beams with different LET values (13, 30 and 50 keV/μm), and chromosomal DNA DSBs were analyzed with FAR assays using SFGE. AA8 cells were also irradiated at room temperature, and survival was measured with colony formation assays. A) Variation of the yield of released DNA with the type of radiation. Data are from a single experiment. B) Cell survival after irradiation with carbon ion beams with the indicated LET values (13, 30 and 50 keV/μm).

decreased with increasing LET (Fig. 7A), whereas the cell killing efficiency increased with increasing LET (Fig. 7B). These results indicate that the decrease in the yield of DSBs, a representative clustered damage, with increasing LET is not peculiar to *in vitro* irradiation of DNA but is common to *in vitro* and *in vivo* irradiation of DNA.

DISCUSSION

In the present study, the formation of isolated DNA damage and bistranded clustered DNA damage was analyzed after the irradiation of two types of DNA (supercoiled pDEL19 plasmid and linear lambda DNA) with different types of radiation. The experiments with plasmid and lambda DNA gave essentially consistent results with respect to the yields and spectra of isolated and clustered damage, although the experiments with lambda DNA tended to give higher estimates of clustered damage than those with plasmid DNA (Figs. 2B and 3B). First, the spectra of isolated and clustered damage were virtually independent of the quality of radiation (γ-rays, carbon ion, and iron ion beams) (Figs. 2D, 2E, 3D, and 3E). Second, the yields of clustered damage, as well as those of isolated damage, decreased with the different types of radiation used in the order γ > C > Fe (Figs. 2A, 2B, 3A, and 3B), and hence exhibited an inverse correlation with LET [0.2 keV/μm (γ), 13 keV/μm (C), and 200 keV/μm (Fe)]. In addition, the observed decreases in the yields of damage were associated with all damage components (Tables 1 and 2). This result is consistent with previous reports showing that the yields of DSBs and oxidized purines and abasic clusters in T7 DNA decreased with increasing LET values of the incident charged particles,[17] and that the yields of oxidized bases (probably primarily isolated lesions) in mammalian cells tended to decrease with increasing LET values.[14] Among the indirect effects of radiation under aerobic conditions, the primary radical responsible for DNA damage induction is the highly reactive hydroxyl radical produced by the radiolysis of water. It has been demonstrated that the yield of hydroxyl radicals (G-value) decreases significantly with increasing LET (G-values are about 2 and 0.3 at 1 and 100 keV/μm, respectively) due to an inactivating recombination of radicals in the spur.[28,29] Thus, there is a good correlation between the variation of the yield of hydroxyl radicals and those of isolated and clustered damage. However, it appears that the LET-dependent variation of damage formation does not stem solely from hydroxyl radical formation. An extrapolation of the published data indicates that the yield of hydroxyl radicals decreases approximately 10-fold over the LET range for γ-rays and iron ions,[28] yet the observed decrease in the damage yields were notably lower than this: 2.5–4.6-fold and 2.0–2.2-fold for total isolated and clustered damage, respectively (Tables 1 and 2). Probably it is necessary to include the contributions stemming from the direct effect of ionizing radiation to be able to fully account for the observations in the present study where DNA was irradiated under radical scavenging conditions.

Regarding the effect of scavenging conditions on damage formation, we have previously shown that the relative yields of DNA damage are 1,052 (DNA irradiated in 10 mM PB) : 18 (DNA irradiated in 10 mM Tris) : 1 (irradiated HeLa cells) when DNA or cells were irradiated by γ-rays.[23] These figures indicate that 98.3% and 99.9% of diffusible OH radicals are scavenged in 10 mM Tris and cells, respectively. Thus, the scavenging capacity of 10 mM Tris for diffusible OH radicals are fairly strong, though it is not completely

equivalent to that of cells. The question is whether a further 10-fold reduction in the amount of remaining OH radicals under cell mimetic conditions would lead to radiation quality-dependent or LET-dependent increases in the yield of clustered damage (or absence thereof) as opposed to the present observation. Our *in vivo* experimental data for DSB formation (Figs. 6 and 7) argue against this possibility. The decrease in the yield of clustered damage with increasing LET was not peculiar to *in vitro* irradiation of DNA but was also observed for chromosomal DNA DSBs in irradiated cells, suggesting that this trend is independent of the microenvironment of DNA. In view of the present *in vitro* and *in vivo* data showing a similar trend with respect to the formation of clustered damage, it might be reasonable to conclude that the higher LET induced lower yield of the clustered damage. The reason is partly due to recombination between OH radicals in the spar as mentioned above.

Three types of clustered damage were quantified, including DSBs, oxidized pyrimidine clusters, and oxidized purine clusters in the present study. The quantitation of DSBs was straightforward and based on the direct measurement of the Type III fraction (plasmid DNA) or size dispersion (lambda DNA) observed in irradiated DNA, indicating that the yield of DSBs determined here represents the one actually present in irradiated DNA. Conversely, the quantitation of oxidized base clusters was indirect and was based on the conversion of these lesions to DSBs by Endo III or Fpg. Accordingly, unlike DSBs, the yields of oxidized base clusters intrinsically depends on the enzymatic conversion efficiency. To maximize the quantitative conversion of oxidized base clusters, the optimal amounts of Endo III and Fpg to use for irradiated DNA was determined by titration, and saturating quantities of enzymes were used. In addition, the validity and limits of the present assays using DNA substrates were assessed using model oxidized base clusters. The results showed that except for –1 and +1 clusters, other configurations could be converted to DSBs under exhaustive digestion conditions (enzyme concentration = 1000 nM, Fig. 5B). Previous studies also showed that clustered base damages with –1 and +1 configurations were resistant to Endo III and Fpg.[27] It is difficult to assess how much these –1 and +1 clusters contribute to the underestimation of the yields of oxidized pyrimidine and purine clusters in the present study, since no experimental data are available regarding their formation in irradiated DNA and their LET dependence. For the production of a –1 or +1 cluster, two damaging events have to occur in adjacent base pairs that occupy only one tenth of a helical turn in DNA. Even considering the actual spatial arrangement of two damaged bases for a –1 or +1 cluster (*e.g.*, Fig. 3A), the inter-base distance is at most 1 nm. Computational simulation of DNA damage formation by low and high LET radiation suggests that all types of radiation produce complex clustered damage such as DSBs with additional proximal breaks or base lesions, and that the proportion of complex clustered damage and the degree of complexity increases with high LET radiation.[30–32] Although these simulation data have provided useful insight into the structure of clustered damage, it is difficult to deduce from these data how the yield of –1 and +1 clusters varies depending on the incident particles and LET. Together with the assessment by computational simulation, it is crucial to corroborate these data by experimental observation.

The present results suggest that the initial yield of clustered DNA damage does not simply account for the adverse biological effect of the ionizing radiation or the variation of RBE with LET. Quantifying clustered damage as either prompt or as glycosylase-induced DSBs is a widely used technique and has provided valuable insights into the nature of potentially detrimental clustered damage induced by ionizing radiation. However, the shortcoming of this approach is that it does not reveal the complexity of clustered damage which may vary with the quality of ionizing radiation, though it does reveal the (approximate) quantity of clustered damage. As mentioned above, computational simulations of DNA damage formation suggest that the proportion of complex clustered damage and the degree of complexity will increase for high LET radiations.[30–32] The structural complexity predicted for radiation-induced clustered damage has been experimentally supported by recent model studies which showed the damage clustering of abasic sites or base lesions within 8 bases of the ^{125}I-targeted bases in duplex DNA.[33,34] It should be noted that the influence of complex clustered damage will emerge only in a repair-proficient background. The RBE increases with increasing LET values up to certain values depending on cell types and endpoints in DSB repair proficient cells, but not in repair deficient cells. Bacterial and mammalian cells deficient in DSB repair do not exhibit LET dependent variations of RBE,[35,36] suggesting that both simple and complex clustered damages are equally crucial in the absence of DSB repair. In future studies, it will be important to devise a method that experimentally allows the assessment of the structural complexity of clustered damage at the sequence level. In addition, it is also essential to determine how much complex clustered damage is refractory to repair and is associated with error prone repair, thereby leading to adverse biological consequences as compared to simple clustered damage.

ACKNOWLEDGEMENTS

The authors thank Dr. Yoshiko Kubota (Iwate Medical University) for a generous gift of AA8 cells and Dr. Ritsuko Watanabe (Japan Atomic Energy Agency) for valuable discussion. This work was supported in part by a Grant-in-Aid from the Ministry of Education, Culture, Sports, Science and Technology (H. I.), The Ground-based Research Announcement for Space Utilization promoted by the Japan Space Forum (H. I.), and the Special Coordination Funds for

Research Projects with Heavy Ions at the National Institute of Radiological Sciences-Heavy-Ion Medical Accelerator in Chiba (NIRS-HIMAC).

REFERENCES

1. Wallace, S. S. (2002) Biological consequences of free radical-damaged DNA bases. Free Radic. Biol. Med., **33**: 1–14.
2. Ward, J. F. (1994) The complexity of DNA damage: relevance to biological consequences. Int. J. Radiat. Biol., **66**: 427–432.
3. Goodhead, D. T. (1994) Initial events in the cellular effects of ionizing radiations: clustered damage in DNA. Int. J. Radiat. Biol., **65**: 7–17.
4. Terato, H. and Ide, H. (2004) Clustered DNA damage induced by heavy ion particles. Biol. Sci. Space, **18**: 206–215.
5. Foray, N., Arlett, C. F. and Malaise, E. P. (1997) Radiation-induced DNA double-strand breaks and the radiosensitivity of human cells: a closer look. Biochimie, **79**: 567–575.
6. Sutherland, B. M., Bennett, P. V., Sidorkina, O. and Laval, J. (2000) Clustered DNA damages induced in isolated DNA and in human cells by low doses of ionizing radiation. Proc. Natl. Acad. Sci. U. S. A., **97**: 103–108.
7. Georgakilas, A. G., Bennett, P. V. and Sutherland, B. M. (2002) High efficiency detection of bi-stranded abasic clusters in gamma-irradiated DNA by putrescine. Nucleic Acids Res., **30**: 2800–2808.
8. Chaudhry, M. A. and Weinfeld, M. (1995) The action of Escherichia coli endonuclease III on multiply damaged sites in DNA. J. Mol. Biol., **249**: 914–922.
9. Harrison, L., Hatahet, Z., Purmal, A. A. and Wallace, S. S. (1998) Multiply damaged sites in DNA: interactions with Escherichia coli endonucleases III and VIII. Nucleic Acids Res., **26**: 932–941.
10. Lomax, M. E., Cunniffe, S. and O'Neill, P. (2004) Efficiency of repair of an abasic site within DNA clustered damage sites by mammalian cell nuclear extracts. Biochemistry, **43**: 11017–11026.
11. Yang, N., Galick, H. and Wallace, S. S. (2004) Attempted base excision repair of ionizing radiation damage in human lymphoblastoid cells produces lethal and mutagenic double strand breaks. DNA Repair, **3**: 1323–1334.
12. Goodhead, D. T. (2006) Energy deposition stochastics and track structure: what about the target? Radiat. Prot. Dosimetry, **122**: 3–15.
13. Prise, K. M., Ahnstrom, G., Belli, M., Carlsson, J., Frankenberg, D., Kiefer, J., Lobrich, M., Michael, B. D., Nygren, J., Simone, G. and Stenerlow, B. (1998) A review of dsb induction data for varying quality radiations. Int. J. Radiat. Biol., **74**: 173–184.
14. Pouget, J. P., Frelon, S., Ravanat, J. L., Testard, I., Odin, F. and Cadet, J. (2002) Formation of modified DNA bases in cells exposed either to gamma radiation or to high-LET particles. Radiat. Res., **157**: 589–595.
15. Prise, K. M., Pullar, C. H. and Michael, B. D. (1999) A study of endonuclease III-sensitive sites in irradiated DNA: detection of alpha-particle-induced oxidative damage. Carcinogenesis, **20**: 905–909.
16. Milligan, J. R., Aguilera, J. A., Paglinawan, R. A., Ward, J. F. and Limoli, C. L. (2001) DNA strand break yields after post-high LET irradiation incubation with endonuclease-III and evidence for hydroxyl radical clustering. Int. J. Radiat. Biol., **77**: 155–164.
17. Hada, M. and Sutherland, B. M. (2006) Spectrum of complex DNA damages depends on the incident radiation. Radiat. Res., **165**: 223–230.
18. Asagoshi, K., Yamada, T., Terato, H., Ohyama, Y., Monden, Y., Arai, T., Nishimura, S., Aburatani, H., Lindahl, T. and Ide, H. (2000) Distinct repair activities of human 7,8-dihydro-8-oxoguanine DNA glycosylase and formamidopyrimidine DNA glycosylase for formamidopyrimidine and 7,8-dihydro-8-oxoguanine. J. Biol. Chem., **275**: 4956–4964.
19. Asagoshi, K., Yamada, T., Okada, Y., Terato, H., Ohyama, Y., Seki, S. and Ide, H. (2000) Recognition of formamidopyrimidine by Escherichia coli and mammalian thymine glycol glycosylases. Distinctive paired base effects and biological and mechanistic implications. J. Biol. Chem., **275**: 24781–24786.
20. Iwai, S. (2001) Synthesis and thermodynamic studies of oligonucleotides containing the two isomers of thymine glycol. Chemistry, **7**: 4343–4351.
21. Sutherland, B. M., Bennett, P. V., Sidorkina, O. and Laval, J. (2000) Clustered damages and total lesions induced in DNA by ionizing radiation: oxidized bases and strand breaks. Biochemistry, **39**: 8026–8031.
22. Ide, H., Akamatsu, K., Kimura, Y., Michiue, K., Makino, K., Asaeda, A., Takamori, Y. and Kubo, K. (1993) Synthesis and damage specificity of a novel probe for the detection of abasic sites in DNA. Biochemistry, **32**: 8276–8283.
23. Ali, M. M., Kurisu, S., Yoshioka, Y., Terato, H., Ohyama, Y., Kubo, K. and Ide, H. (2004) Detection of endonuclease III- and 8-oxoguanine glycosylase-sensitive base modifications in gamma-irradiated DNA and cells by the aldehyde reactive probe (ARP) assay. J. Radiat. Res., **45**: 229–237.
24. Schneider, M., Taucher-Scholz, G., Heilmann, J. and Kraft, G. (1994) Combination of static-field gel electrophoresis and densitometric scanning for the determination of radiation-induced DNA double-strand breaks in CHO cells. Radiat. Environ. Biophys., **33**: 111–124.
25. Hirayama, R., Furusawa, Y., Fukawa, T. and Ando, K. (2005) Repair kinetics of DNA-DSB induced by X-rays or carbon ions under oxic and hypoxic conditions. J. Radiat. Res., **46**: 325–332.
26. Ide, H. (2001) DNA substrates containing defined oxidative base lesions and their application to study substrate specificities of base excision repair enzymes. Prog. Nucleic Acid Res. Mol. Biol., **68**: 207–221.
27. Blaisdell, J. O., Harrison, L. and Wallace, S. S. (2001) Base excision repair processing of radiation-induced clustered DNA lesions. Radiat. Prot. Dosimetry, **97**: 25–31.
28. Burns, W. G. and Sims, H. E. (1981) Effect of radiation type in water radiolysis. J. Chem. Soc. Faraday Trans. 1, **77**: 2803–2813.
29. Gervais, B., Beuve, M., Olivera, G. H. and Galassi, M. E. (2006) Numerical simulation of multiple ionization and high LET effects in liquid water radiolysis. Radiat. Phys. Chem., **75**: 493–513.

30. Nikjoo, H., O'Neill, P., Goodhead, D. T. and Terrissol, M. (1997) Computational modelling of low-energy electron-induced DNA damage by early physical and chemical events. Int. J. Radiat. Biol., **71**: 467–483.
31. Nikjoo, H., O'Neill, P., Wilson, W. E. and Goodhead, D. T. (2001) Computational approach for determining the spectrum of DNA damage induced by ionizing radiation. Radiat. Res., **156**: 577–583.
32. Nikjoo, H., Bolton, C. E., Watanabe, R., Terrissol, M., O'Neill, P. and Goodhead, D. T. (2002) Modelling of DNA damage induced by energetic electrons (100 eV to 100 keV). Radiat. Prot. Dosimetry, **99**: 77–80.
33. Datta, K., Neumann, R. D. and Winters, T. A. (2005) Characterization of complex apurinic/apyrimidinic-site clustering associated with an authentic site-specific radiation-induced DNA double-strand break. Proc. Natl. Acad. Sci. U. S. A., **102**: 10569–10574.
34. Datta, K., Jaruga, P., Dizdaroglu, M., Neumann, R. D. and Winters, T. A. (2006) Molecular analysis of base damage clustering associated with a site-specific radiation-induced DNA double-strand break. Radiat. Res., **166**: 767–781.
35. Munson, R. J., Neary, G. J., Bridges, B. A. and Preston, R. J. (1967) The sensitivity of Escherichia coli to ionizing particles of different LETs. Int. J. Radiat. Biol. Relat. Stud. Phys. Chem. Med., **13**: 205–224.
36. Weyrather, W. K., Ritter, S., Scholz, M. and Kraft, G. (1999) RBE for carbon track-segment irradiation in cell lines of differing repair capacity. Int. J. Radiat. Biol., **75**: 1357–1364.

Received on September 6, 2007
Revision received on October 31, 2007
Accepted on November 2, 2007
J-STAGE Advance Publication Date: January 24, 2008